PROOF COVER SHEET

Author(s):	Abhishek Gupta, Wan Li Low, Iza Radecka, Stephen T. Britland, Mohd Cairul Iqbal Mohd Amin, and Claire Martin
Article title:	Characterisation and *in vitro* antimicrobial activity of biosynthetic silver-loaded bacterial cellulose hydrogels
Article no:	IMNC_A_1253796
Enclosures:	1) Query sheet 2) Article proofs

Dear Author,

1. Please check these proofs carefully. It is the responsibility of the corresponding author to check these and approve or amend them. A second proof is not normally provided. Taylor & Francis cannot be held responsible for uncorrected errors, even if introduced during the production process. Once your corrections have been added to the article, it will be considered ready for publication.

Please limit changes at this stage to the correction of errors. You should not make trivial changes, improve prose style, add new material, or delete existing material at this stage. You may be charged if your corrections are excessive (we would not expect corrections to exceed 30 changes).

For detailed guidance on how to check your proofs, please paste this address into a new browser window: http://journalauthors.tandf.co.uk/production/checkingproofs.asp

Your PDF proof file has been enabled so that you can comment on the proof directly using Adobe Acrobat. If you wish to do this, please save the file to your hard disk first. For further information on marking corrections using Acrobat, please paste this address into a new browser window: http://journalauthors.tandf.co.uk/production/acrobat.asp

2. Please review the table of contributors below and confirm that the first and last names are structured correctly and that the authors are listed in the correct order of contribution. This check is to ensure that your name will appear correctly online and when the article is indexed.

Sequence	Prefix	Given name(s)	Surname	Suffix
1		Abhishek	Gupta	
2		Wan Li	Low	
3		Iza	Radecka	
4		Stephen T.	Britland	
5		Mohd Cairul Iqbal	Mohd Amin	
6		Claire	Martin	

Queries are marked in the margins of the proofs, and you can also click the hyperlinks below.

General points:

1. **Permissions:** You have warranted that you have secured the necessary written permission from the appropriate copyright owner for the reproduction of any text, illustration, or other material in your article. Please see http://journalauthors.tandf.co.uk/permissions/usingThirdPartyMaterial.asp.

2. **Third-party content:** If there is third-party content in your article, please check that the rightsholder details for re-use are shown correctly.

3. **Affiliation:** The corresponding author is responsible for ensuring that address and email details are correct for all the co-authors. Affiliations given in the article should be the affiliation at the time the research was conducted. Please see http://journalauthors.tandf.co.uk/preparation/writing.asp.

4. **Funding:** Was your research for this article funded by a funding agency? If so, please insert `This work was supported by <insert the name of the funding agency in full>', followed by the grant number in square brackets `[grant number xxxx]'.
5. **Supplemental data and underlying research materials:** Do you wish to include the location of the underlying research materials (e.g. data, samples or models) for your article? If so, please insert this sentence before the reference section: `The underlying research materials for this article can be accessed at <full link>/ description of location [author to complete]'. If your article includes supplemental data, the link will also be provided in this paragraph. See <http://journalauthors.tandf.co.uk/preparation/multimedia.asp> for further explanation of supplemental data and underlying research materials.

6. The **PubMed** (http://www.ncbi.nlm.nih.gov/pubmed) and **CrossRef databases** (www.crossref.org/) have been used to validate the references. Changes resulting from mismatches are tracked in red font.

AUTHOR QUERIES

Q1: Please provide the town and state abbreviation (for US) or town and country of origin (for other countries) identifying the headquarter location for "Acros Organics".
Q2: A disclosure statement reporting no conflict has been inserted. Please confirm the statement is accurate.
Q3: Please provide complete details for (Solway and Consalter, 2010) in the reference list or delete the citation from the text.
Q4: Please check reference Costa and Lobo (2001) in the text citation is changed to Costa and Lobo (2011) as per reference list.
Q5: Please provide the page range for Ref. (Kim et al. 2009) in the reference list entry.
Q6: Please provide the page range for Ref. (Murphy & Evans, 2012) in the reference list entry.
Q7: The ORCID details of the authors have been validated against ORCID registry. please check the ORCID ID details of the authors.
Q8: Please check and confirm the corresponding author details correct as set in proof.
Q9: Please resupply Figures 3 and 4 in a format suitable for printing.

How to make corrections to your proofs using Adobe Acrobat/Reader

Taylor & Francis offers you a choice of options to help you make corrections to your proofs. Your PDF proof file has been enabled so that you can mark up the proof directly using Adobe Acrobat/Reader. This is the simplest and best way for you to ensure that your corrections will be incorporated. If you wish to do this, please follow these instructions:

1. Save the file to your hard disk.

2. Check which version of Adobe Acrobat/Reader you have on your computer. You can do this by clicking on the Help" tab, and then About".

If Adobe Reader is not installed, you can get the latest version free from http://get.adobe.com/reader/.

3. If you have Adobe Acrobat/Reader 10 or a later version, click on the Comment" link at the right-hand side to view the Comments pane.

4. You can then select any text and mark it up for deletion or replacement, or insert new text as needed. Please note that these will clearly be displayed in the Comments pane and secondary annotation is not needed to draw attention to your corrections. If you need to include new sections of text, it is also possible to add a comment to the proofs. To do this, use the Sticky Note tool in the task bar. Please also see our FAQs here: http://journalauthors.tandf.co.uk/production/index.asp.

5. Make sure that you save the file when you close the document before uploading it to CATS using the Upload File" button on the online correction form. If you have more than one file, please zip them together and then upload the zip file.
If you prefer, you can make your corrections using the CATS online correction form.

Troubleshooting

Acrobat help: http://helpx.adobe.com/acrobat.html
Reader help: http://helpx.adobe.com/reader.html

Please note that full user guides for earlier versions of these programs are available from the Adobe Help pages by clicking on the link Previous versions" under the Help and tutorials" heading from the relevant link above. Commenting functionality is available from Adobe Reader 8.0 onwards and from Adobe Acrobat 7.0 onwards.

Firefox users: Firefox's inbuilt PDF Viewer is set to the default; please see the following for instructions on how to use this and download the PDF to your hard drive: http://support.mozilla.org/en-US/kb/view-pdf-files-firefox-without-downloading-them#-w_using-a-pdf-reader-plugin

JOURNAL OF MICROENCAPSULATION, 2016
http://dx.doi.org/10.1080/02652048.2016.1253796

Taylor & Francis
Taylor & Francis Group

RESEARCH ARTICLE

Characterisation and *in vitro* antimicrobial activity of biosynthetic silver-loaded bacterial cellulose hydrogels

Abhishek Gupta[a,c], Wan Li Low[a,c], Iza Radecka[b,c], Stephen T. Britland[a,c], Mohd Cairul Iqbal Mohd Amin[d] and Claire Martin[a,c]

[a]School of Pharmacy, Faculty of Science and Engineering, University of Wolverhampton, Wolverhampton, UK; [b]School of Biology, Chemistry and Forensic Science, Faculty of Science and Engineering, University of Wolverhampton, Wolverhampton, UK; [c]Research Institute in Healthcare Science, Faculty of Science and Engineering, University of Wolverhampton, Wolverhampton, UK; [d]Faculty of Pharmacy, Universiti Kebangsaan Malaysia, Kuala Lumpur, Malaysia

ABSTRACT

Wounds that remain in the inflammatory phase for a prolonged period of time are likely to be colonised and infected by a range of commensal and pathogenic microorganisms. Treatment associated with these types of wounds mainly focuses on controlling infection and providing an optimum environment capable of facilitating re-epithelialisation, thus promoting wound healing. Hydrogels have attracted vast interest as moist wound-responsive dressing materials. In the current study, biosynthetic bacterial cellulose hydrogels synthesised by *Gluconacetobacter xylinus* and subsequently loaded with silver were characterised and investigated for their antimicrobial activity against two representative wound infecting pathogens, namely *S. aureus* and *P. aeruginosa*. Silver nitrate and silver zeolite provided the source of silver and loading parameters were optimised based on experimental findings. The results indicate that both $AgNO_3$ and AgZ loaded biosynthetic hydrogels possess antimicrobial activity ($p < .05$) against both *S. aureus* and *P. aeruginosa* and may therefore be suitable for wound management applications.

ARTICLE HISTORY
Received 18 July 2016
Revised 17 October 2016
Accepted 17 October 2016
Published online ▮▮▮

KEYWORDS
Antimicrobial; bacterial cellulose; hydrogel; silver; silver zeolite

Introduction

Wound healing is a complex physiological cascade that follows several orderly, but overlapping phases (Guo and DiPietro, 2010; Martin et al., 2014), the rate of which is influenced by the type, size and depth of wound, as well as the presence of infection (Martin et al., 2013). Invasion of endogenous or exogenous pathogenic microorganisms into the wound site (Landis, 2008) can delay normal wound healing and potentially lead to the development of a chronic, non-healing wound. This microbial invasion usually occurs due to the uncontrolled proliferation of opportunistic pathogens amongst the polymicrobial skin microflora: Opportunistic microorganisms (e.g. *Streptococcus* spp, *Corynebacterium* spp, *Escherichia coli*, *Bacillus subtilis*, *Staphylococcus aureus* and *Pseudomonas aeruginosa*) can colonise the wound site and substantially prolong wound healing (Kirketerp-Møller et al., 2008; Landis, 2008). Conventional dressings (e.g. gauze and tulle) form a barrier from the external environment and keep the wound dry, but are unable to directly influence the healing process (Singh et al., 2013; Kamoun et al., 2015). Conversely, moist dressings act as a barrier to infection and also maintain moisture levels around the wound. These dressings are easily removed from the wound site, thus avoiding further trauma during dressing changes, and in the case of hydrogel-based dressings, respond to variations in moisture, thereby facilitating re-epithelialisation (Winter, 1962; Abdelrahman and Newton, 2011; Fu et al., 2013). In addition to absorbing and retaining wound exudate, hydrogel-based dressings also provide a cooling, soothing effect, thereby reducing the sensation of pain (Maneerung et al., 2008; Solway ~~and Consalter,~~ 2010).

Bacterial cellulose (BC), a biosynthetic homopolymer synthesised by the Gram negative obligate aerobe *Gluconacetobacter xylinus* (Pinto et al., 2009; Castro et al., 2011) has attracted great interest as a potential wound dressing (Czaja et al., 2006; Solway et al., 2010). Unlike plant cellulose, BC is highly pure and free from contaminants such as lignin, pectin and hemicellulose (Sannino et al., 2009); its highly crystallised microstructure also results in a finer web-like network with higher tensile strength compared to plant cellulose (Pinto et al., 2009). BC is biocompatible, non-pyrogenic, hydrophilic and transparent, all of which make it innately suitable for wound management applications (Czaja et al., 2006; Fu et al., 2013; Abeer et al., 2014). The hydrophilicity and relatively high swelling ratio of BC (Nakayama et al., 2004; Maneerung et al., 2008) allow it to establish a moist microenvironment at the wound interface in addition to maintaining water vapour transmission rate (WVTR) and a constant temperature. Hydrophilicity also enables reversible swelling and de-swelling of the hydrogel, which can be exploited in the fluid management of heavily exuding wounds. In addition, BC hydrogel dressings can protect tissues forming over and around the wound site, as well as promote angiogenesis (Maneerung et al., 2008). These unique properties have led to the successful commercialisation of BC hydrogels (e.g. Dermafill™, Biofill®, Bioprocess® and Gengiflex®) for the treatment of burns, chronic ulcers, skin lesions and periodontal disease, respectively (Czaja et al., 2006; Solway et al., 2010; Fu et al., 2013). Whilst not inherently antimicrobial itself, BC's unique 3-D nanofibrillar network is highly porous and amenable to high loading and controlled release of a range of antimicrobial agents (Fu et al., 2013; Shah et al., 2013; Wu et al., 2014).

CONTACT Claire Martin claire.martin2@wlv.ac.uk School of Pharmacy, Faculty of Science and Engineering, University of Wolverhampton, Wolverhampton, UK

Ionic silver (Ag^+) is a broad spectrum antimicrobial agent with activity against yeast, fungi and several antibiotic resistant bacteria including methicillin resistant *S. aureus* (MRSA) and vancomycin resistant enterococci (VRE) (Murphy and Evans, 2012). Of equal importance, Ag^+ has relatively low toxicity in human cells at concentrations that are antimicrobially active against pathogenic microbes (Copcia et al., 2011; Wilkinson et al., 2011). Since the dawn of the antibiotic era, the use of Ag^+ has gradually decreased, but the upsurge in multidrug resistant microbial strains has led to a resurgence in interest (Chopra, 2007; Radecka et al., 2015). Ag^+ are highly reactive and can bind to multiple intra- and extracellular target sites that alter cellular functionality, structural integrity, permeability and transport systems (Chopra, 2007; Maneerung et al., 2008; Low et al., 2013; Martin et al., 2013; Martin et al., 2015). Once transported into the bacterial cytoplasm, Ag^+ interact with essential intracellular enzymes and DNA, disrupting vital cell functions and impairing cell replication, that eventually lead to cell death (Castellano et al., 2007; Low et al., 2011; Low et al., 2013; Martin et al., 2015). The multifaceted, broad spectrum mode of action of Ag^+ can be highly effective at controlling chronic wound infections even at parts per million concentrations (Brett, 2006). The minimum lethal concentration (MLC) of Ag^+ against *P. aeruginosa* and *S. aureus* was reported to be $1.59 \times 10^{-3\%}$ w/v (equivalent to 15.9 ppm) and $5.08 \times 10^{-3\%}$ w/v (equivalent to 50.8 ppm) respectively (Low et al., 2011). Silver has other beneficial wound management functions including anti-inflammatory activity resulting from complex formation with metalloproteinases, leading to localised down regulation of inflammation, thus creating conditions suitable for re-epithelialisation and angiogenesis (Atiyeh et al., 2007; Leaper, 2012). There are several commercially available topical silver products including dressings (Acticoat®, Contreet-H®, Actisorb Silver 220®, Aquacel-Ag®, Ag Extra™), solutions (Sulfamylon®) and creams (Silvadene®, Flamazine™) (Martin et al., 2013). Whilst the most commonly used products contain silver nitrate or silver sulfadiazine as the source of Ag^+ (Ip et al., 2006), an alternative donor of Ag^+ are silver zeolites (AgZ): a microporous, non-reactive, crystalline aluminosilicate frameworks containing Ag^+ (Kwakye-Awuah et al., 2008). The anionic cavities of zeolites are occupied by cations and/or water molecules that have considerable freedom of movement that permit charge balancing ions to exchange in aqueous media, without affecting the structure of zeolites (Copcia et al., 2011). Cationic Ag^+ interacts with the anionic zeolite framework to form AgZ; the subsequent release of Ag^+ from the zeolite structure is achieved by cation exchange (Kwakye-Awuah et al., 2013). The antimicrobial activity of AgZ has been attributed to Ag^+ release from the zeolite, and the subsequent formation of reactive oxygen species in the matrix (Matsumura et al., 2003). Kwakye-Awuah et al. (2013) and Matsumura et al. (2003) have demonstrated the antimicrobial activity of AgZ against Gram positive (*S. aureus*) and Gram negative (*E. coli* and *P. aeruginosa*) bacteria, all of which are commonly found in infected wounds.

The combination of silver and BC is not extensively reported in the literature: Maneerung et al. (2008), Yang et al. (2012) and Wu et al. (2014) reported the antimicrobial activity of silver nanoparticle-impregnated BC against *E. coli* (Gram negative) and *P. aeruginosa* (Gram positive). Antimicrobial silver-impregnated cellulose (SIC) was microbiocidal against *P. putida* and *M. luteus*, and demonstrated growth inhibition against *C. albicans* and *E. coli* (Kim et al., 2009). With the aim of exploring the effect of silver ion donor type on Ag^+ release and antimicrobial performance, we describe here the characterisation of biosynthetic BC hydrogels loaded with two forms of silver ($AgNO_3$ or AgZ) and establish their *in vitro* antimicrobial activity against the common wound infecting pathogens, *S. aureus* and *P. aeruginosa*.

Material and methods

Microorganisms

G. xylinus ATCC 23770, *P. aeruginosa* NCIMB 8295 and *S. aureus* NCIMB 6571 were obtained from the University of Wolverhampton culture collection. All three microorganisms were maintained at −20 °C in a freeze-dried form. Stock cultures of *P. aeruginosa* and *S. aureus* were resuscitated on sterile tryptone soy agar (TSA, prepared according to the manufacturer's protocol and sterilised by autoclaving before use) (Sigma-Aldrich, Irvine, UK), and incubated for 48 h at 37 °C. Stock culture of *G. xylinus* was resuscitated on sterile mannitol agar (composition: yeast extract (5 g/L), peptone (3 g/L), mannitol (25 g/L), agar (15 g/L); all materials were purchased from Lab M, Bury, UK) and incubated at 48 h at 30 °C. Prior to experimental use, overnight broth cultures were aseptically prepared in suitable broth using the stock plates.

Microbiological media

Dextrose, bacteriological peptone, yeast extract for the Hestrin and Schramm (HS) culture media were purchased from Lab M (Bury, UK). HS media was prepared following the standard protocol (Hestrin and Schramm, 1954). TSA, tryptone soya broth (TSB) (prepared according to the manufacturer's protocol and sterilised by autoclaving before use), disodium phosphate and citric acid were purchased from Sigma-Aldrich (Irvine, UK).

Materials

Cellulose (microcrystalline form) was purchased from Sigma-Aldrich (Irvine, UK). Zeolites (13X) were purchased from Laporte Inorganics (Widnes, UK) and AgZ were purchased from Sigma-Aldrich (Irvine, UK). Silver nitrate ($AgNO_3$) was from Fisher Scientific (Cramlington, UK) and sodium hydroxide from Acros Organics (UK). Ringer solution (1/4 strength) tablets were purchased from Lab M (Bury, UK) and prepared by dissolving one tablet in 500 mL of de-ionised water with constant magnetic stirring prior to sterilisation. Sterile 24-well tissue culture plates were purchased from Sarstedt (Leicester, UK).

Preparation and purification of BC pellicles

BC hydrogels were biosynthesised at 30 °C, under static conditions by *G. xylinus* in freshly prepared sterile HS culture medium. After 14 days, biosynthetic BC pellicles floated on top of the HS growth medium and after harvesting were purified by boiling in 1% w/v sodium hydroxide to obtain pure BC. The pellicles were further boiled in deionised water until the BC became clear and transparent.

Loading of silver in BC pellicles

Silver nitrate ($AgNO_3$)

The silver content in $AgNO_3$ used in this investigation was 63.5% w/w. BC pellicles were padded dry and loaded with aqueous $AgNO_3$ (0.55% w/v) by overnight incubation with constant agitation at 37 °C. The proportion of Ag^+ in both formulations, i.e. $AgNO_3$ and AgZ was equivalent.

Silver zeolites

The silver content in the commercially available AgZ used in the current study was 35% w/w. After purification, BC pellicles were padded dry on filter paper and loaded with AgZ by overnight immersion in 1% w/v aqueous AgZ suspension at 37 °C under static conditions. It was subsequently noticed that some AgZ settled at the bottom of the vessel during loading, so the above procedure was repeated by immersing freshly purified BC in an aqueous AgZ suspension at 37 °C under constant agitation overnight.

Characterisation of BC and silver loaded BC

Scanning electron microscopy (SEM) and energy dispersive X-ray (EDX) analysis

The samples were freeze dried for 48 h (Christ β 1,8-LSC plus, Martin Christ GmbH, Osterode am Harz, Germany) and coated with an ultrafine gold coating for SEM imaging. The morphology of BC-AgZ loaded under static and agitated conditions as well as BC-$AgNO_3$ was studied using Zeiss Evo®50 EP, SEM (Carl Zeiss AG, Oberkochen, Germany). Samples were also analysed by EDX (Zeiss Evo®50 EP, SEM) to confirm the presence of silver. Prior to analysis, each sample was placed on a stub and sprayed with compressed air to remove any traces of dust which can affect analysis.

Fourier transform infrared (FTIR) spectroscopy

Purified BC was analysed using FTIR spectroscopy (Genesis II FTIR™, Thermo Scientific, Runcorn, UK) by first conducting a background scan followed by a scan of the sample to produce spectra. Pure cellulose, BC-$AgNO_3$ and BC-AgZ were also investigated in a similar way.

Swelling ratio

Swelling behaviour was investigated with BC pellicles (9.25 ± 0.25 cm diameter) that were padded dry and the weight (W_x) recorded. Padded dry pellicles were soaked in 200 mL de-ionised water at 37 °C for 24 h under static conditions. After 24 h, the pellicles were withdrawn from water and the swollen BC gently wiped with filter paper prior to reweighing (W_s). The swelling ratio (conducted in triplicate) was calculated as follows:

$$\text{Swelling ratio} = \frac{W_s - W_x}{W_x}$$

Silver release

Similar sized discs of BC-AgZ, BC-$AgNO_3$ and a negative control of BC loaded with zeolite (BC-Z) (all ≈7.0 mm diameter) were cut using a corer. BC-Z, BC-AgZ and BC-$AgNO_3$ discs were transferred into individual wells of a 24-well tissue culture flat bottom plate, and 1 mL of freshly prepared sterile TSB (release media) was added. Discs were then incubated under static conditions at 37 °C for 96 h, and a 1 mL aliquot of release media withdrawn every 24 h; an equal volume (1 mL) of fresh sterile TSB was added at each time point to maintain sink conditions. Silver release was subsequently assessed by Inductively Coupled Plasma (ICP) spectrometry (Agilent Technologies 5100 ICP-OES, Agilent Technologies Inc., Santa Clara, CA). The kinetics of Ag^+ release from BC-$AgNO_3$ and BC-AgZ were analysed by fitting the ICP data to zero order, first order, Higuichi and Korsmeyer–Peppas equations (Costa and Lobo, ~~2011~~).

Antimicrobial activity

The antimicrobial activity of BC-AgZ (loaded under both static and constantly agitated conditions) and BC-$AgNO_3$ was investigated against *P. aeruginosa* and *S. aureus,* using the disc diffusion assay; purified BC and BC-Z (loaded under constant agitation) were used as controls. Discs of BC-AgZ, BC-$AgNO_3$, BC-Z and BC (≈7.0 mm diameter) were aseptically placed on TSA plates seeded with overnight cultures of *P. aeruginosa* or *S. aureus* and following incubation at 37 °C for 24 h, the zone of inhibition (ZOI) was measured. Individual discs were subsequently transferred onto freshly seeded plates (*P. aeruginosa* or *S. aureus*) to ensure consistent, reproducible microbial growth and incubated again under the same conditions for a further 24 h. Results are presented for ZOI at 24, 48, 72 and 96 h.

Statistical analysis

All experiments were performed in at least triplicate and data presented are means ± standard deviation (SD). Data recorded during the course of experiments were analysed statistically by the analysis of variance (ANOVA) using routines of the statistical software "SPSS 20" (SPSS Inc., Chicago, IL) and the differences between means were compared using the Least Significant Differences (LSD) at 5% level of probability ($p < .05$).

Results

Purification of biosynthetic BC pellicles

BC pellicles harvested after 2 weeks of growth from static HS *G. xylinus* cultures were opaque with extensive brown mottling due to residual media, entrapped bacterial cells and other fermentation debris (Figure 1(a)). After washing once in 1% w/v sodium hydroxide, followed by repeat washing in deionised water, purified pellicles became clear and transparent (Figure 1(b)).

BC-AgZ loading: static versus agitated conditions

Visual inspection of BC-AgZ loaded under static conditions revealed inconsistent loading (Figure 1(c)), where some areas of the BC display a higher AgZ content and others very little. BC-AgZ loaded under constant agitation appears to have a more even distribution of AgZ and hence more consistent loading (Figure 1(d)).

Scanning electron microscopy and EDX

Individual *G. xylinus* produces ribbons of cellulose that become entangled with each other, thus creating a dense network structure. Untreated BC pellicles reveal the presence of bacteria and other fermentation debris entrapped within the cellulose network (Figures 2(a) and 3(a)), but once purified, no bacteria were visible (Figure 2(b)). The purification process was also confirmed by EDX spectra, which indicate the removal of extraneous material from the BC (Figure 3(a,b)). BC pellicles have interwoven thick mats of cellulose fibres ranging between 0.01 and 0.15 μm, that following freeze drying, have a dense, fibrous network interspersed with voids (Figure 2(b)). SEM images of freeze dried BC-AgZ (Figure 2(c,d)) and BC-$AgNO_3$ (Figure 2(e)) revealed AgZ and silver microcrystals entrapped within the dense cellulose network. After loading with AgZ under constant agitation, BC-AgZ displayed more consistent, uniform loading (Figure 2(d)) compared to that prepared under static conditions (Figure 2(c)). The presence of silver in both BC-AgZ and BC-$AgNO_3$ was confirmed by EDX spectra (Figure 3(c,d)). Additionally, the presence of aluminium, silicon as well as elemental traces of calcium, sodium, magnesium and iron was also evident on EDX spectra of BC-AgZ (Figure 3(c)). Clusters of encapsulated AgZ particles ranged from 2.0 to 20.0 μm, with

COLOR Online / B&W in Print

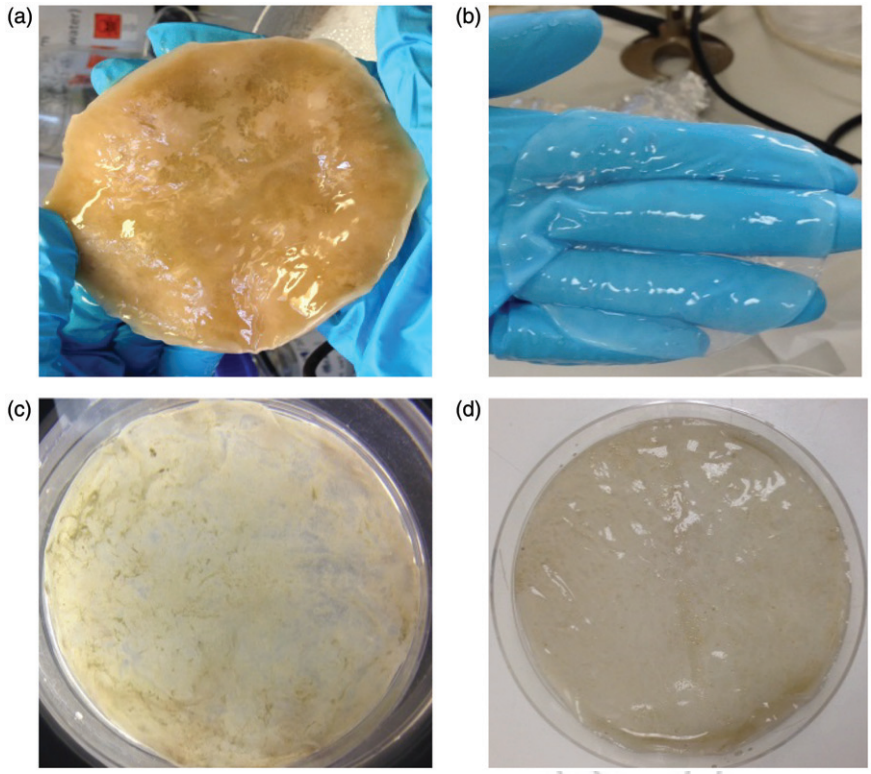

Figure 1. Photographs of (a) untreated BC; (b) purified (washed) BC; silver zeolite-loaded BC (BC-AgZ) under (c) static and (d) agitated conditions.

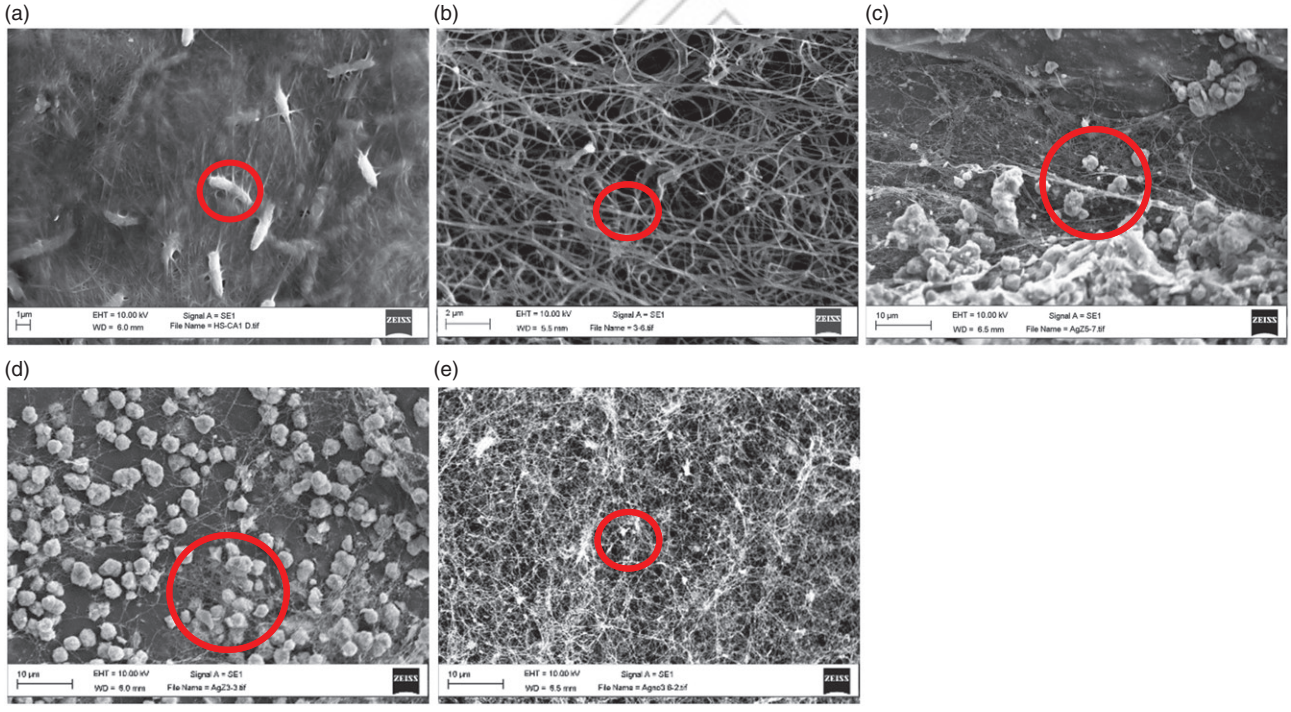

Figure 2. SEM images of (a) untreated BC, entrapped residual *G. xylinus* highlighted; (b) purified BC, fibre network highlighted; (c) BC loaded with AgZ under static conditions, greater density of AgZ highlighted; (d) BC loaded with AgZ under constant agitation, AgZ highlighted, and (e) BC loaded with $AgNO_3$ under constant agitation, $AgNO_3$ impregnated in BC network highlighted.

single AgZ particles (0.5–5.0 μm) also encapsulated within the BC (Figure 2(c,d)). Conversely, crystals of $AgNO_3$ entrapped within the BC fibres had an average range of 0.08–3.5 μm (Figure 2(e)). In summary, the three-dimensional cellulose network consists of a large number of voids that become pores for sequestration of encapsulated silver microcrystals or AgZ when rehydrated.

Fourier transform infrared

The FTIR spectra of a commercially available cellulose sample, purified BC, BC-$AgNO_3$ and BC-AgZ are shown in Figure 4. Similarity in peak characteristics are shown in the spectra for the commercially available cellulose and purified BC at band regions

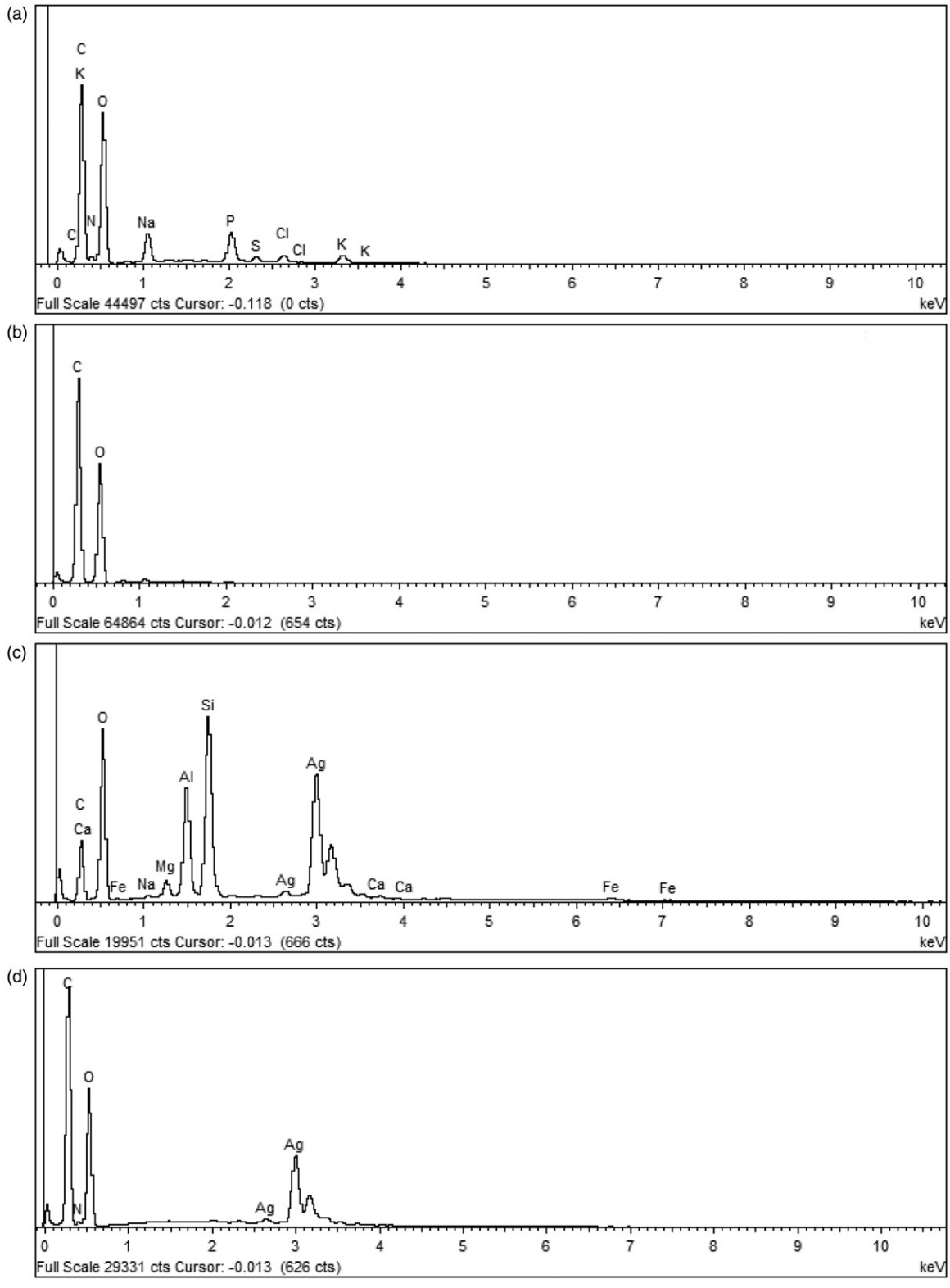

Figure 3. EDX spectra of (a) untreated BC; (b) purified BC; (c) BC loaded with AgZ; and (d) BC loaded with $AgNO_3$.

of 3330 cm^{-1}, 2894 cm^{-1}, 1641 cm^{-1}, 1370 cm^{-1}, 1159 cm^{-1} and 1056 cm^{-1} (Figure 4(a,b)); these peaks were also observed in both the BC-$AgNO_3$ and BC-AgZ spectra (Figure 4(c,d)). The characteristic peaks for $AgNO_3$ (733 cm^{-1}, 803 cm^{-1} and 1300 cm^{-1}) and AgZ (434 cm^{-1}, 553 cm^{-1}, 665 cm^{-1} and 980 cm^{-1}) were also observed in the spectra, thereby confirming the encapsulation of $AgNO_3$ or AgZ within the BC network.

Swelling behaviour

The absorption of surrounding fluids is a vital characteristic of hydrogels for potential application in the management of exudating wounds. After immersion in deionised water, padded dry BC pellicles imbibed an amount of water up to several times its original dehydrated weight, with a swelling ratio of 12.08 ± 0.96 after 24 h.

COLOR Online / B&W in Print

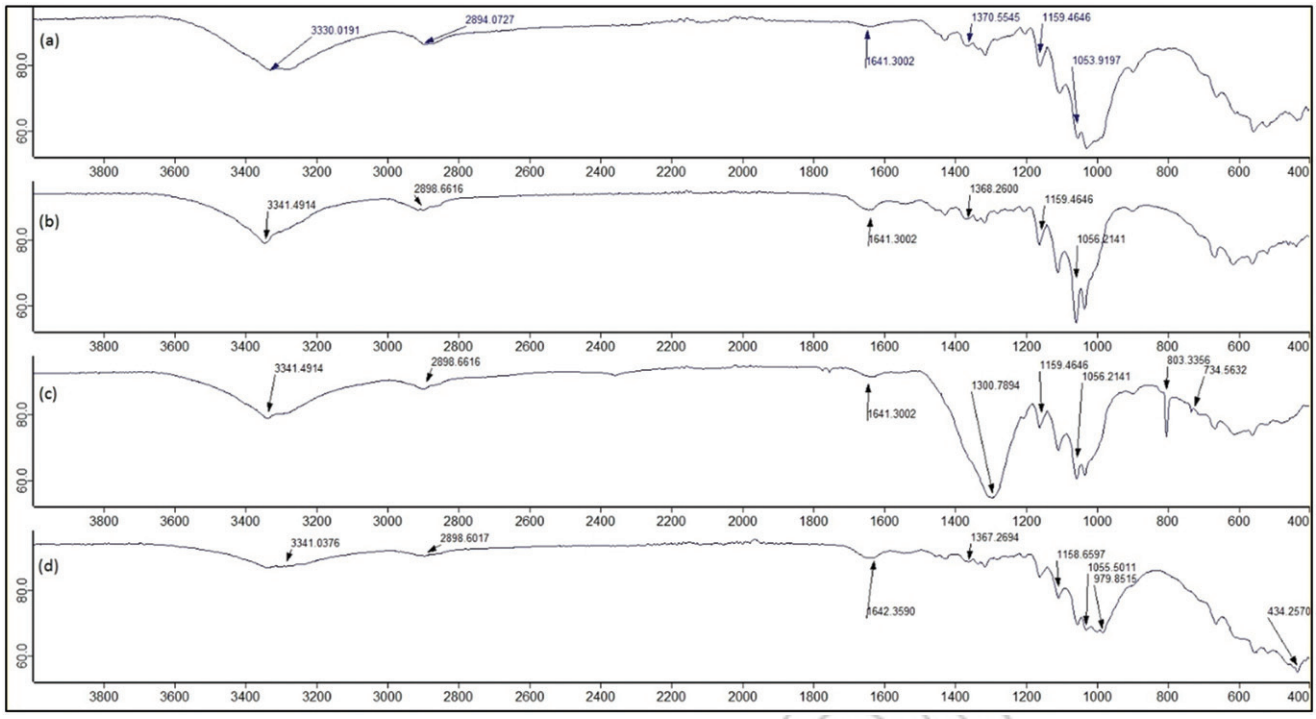

Figure 4. FTIR spectra from 400 to 4000 cm^{-1} for (a) commercially available cellulose; (b) purified BC; (c) BC-$AgNO_3$; and (d) BC-AgZ.

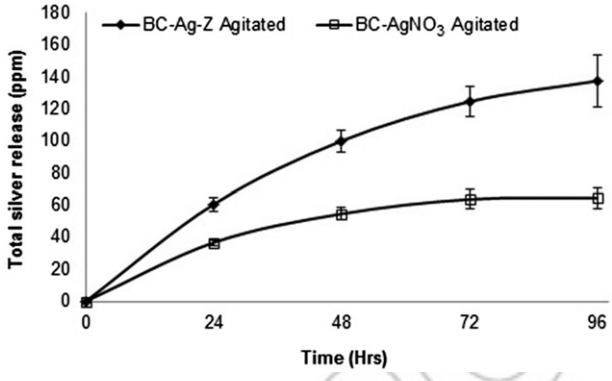

Figure 5. Silver release (ppm) over 96 h from BC-$AgNO_3$ and BC-AgZ as determined by ICP ($n = 4$).

Silver release

Ag^+ release from BC hydrogels, as determined by ICP analysis, is presented in Figure 5. Results indicate that Ag^+ release was greatest after 24 h from BC-AgZ (60.65 ± 4.18 ppm) and BC-$AgNO_3$ (36.76 ± 1.68 ppm). Silver release from BC-$AgNO_3$ plateaued after 72 h whereas from BC-AgZ release was steady and controlled (Figure 5). Overall, BC-AgZ released more silver (137.60 ± 16.17 ppm) over the 96 h compared to BC-$AgNO_3$ (64.53 ± 6.47 ppm).

Mathematical modelling of silver release

When silver release was analysed with zero order, first order, Higuchi and Korsmeyer–Peppas equations, results confirm that BC-AgZ and BC-$AgNO_3$ adhere to the Korsmeyer–Peppas model (Table 1). With a correlation coefficient of >0.97 ($R^2 \geq .99$ for both BC-AgZ and BC-$AgNO_3$) and release exponent between 0.45 and 0.89 (BC-AgZ = 0.73; BC-$AgNO_3$ = 0.56) which indicates that Ag^+ release is non-Fickian (anomalous transport) (Costa and Lobo, 2011; Dash et al., 2010). Interestingly, Ag^+ release from BC-AgZ also follows the Higuichi model with a correlation coefficient of >0.97 (R^2=.99), i.e. diffusional release (Costa and Lobo, 2011). The additional diffusional release of Ag^+ from AgZ at the surface of the BC may be due to ion exchange with cations present in the TSB media. The correlation coefficients for zero and first order models were both <0.97 (Table 1).

Table 1. Mathematical modelling of Ag^+ release kinetics.

	Correlation coefficient (R^2)			
	Zero order	First order	Higuichi	Korsmeyer–Peppas
BC-AgZ	0.93	0.92	0.99	>0.99
BC-$AgNO_3$	0.84	0.69	0.98	0.99

Antimicrobial activity

Pure BC and BC-Z exhibited no antimicrobial activity. There was a difference in antimicrobial activity for AgZ loaded BC *via* static and agitation methods (Figure 6(a,b)). The antimicrobial activity of BC-AgZ loaded under constant agitation was significantly better against *P. aeruginosa* (BC-AgZ (static): 8.29 mm ≤ ZOI ≤14.15 mm; BC-AgZ (agitated): 16.10 mm ≤ ZOI ≤17.96; $p < .05$). However, this was not observed in the case of *S. aureus* when comparing the antimicrobial activity of BC-AgZ loaded under static or agitated condition (BC-AgZ (static): 7.94 mm ≤ ZOI ≤10.31 mm; BC-AgZ (agitated): 7.71 mm ≤ ZOI ≤10.06 mm; $p > .05$).

The disc diffusion assay for antimicrobial activity indicated that both BC-AgZ and BC-$AgNO_3$ exhibited higher antimicrobial activity against *P. aeruginosa* compared to *S. aureus* (Figure 7(a,b)). Statistical analysis using ANOVA suggests that there is a significant difference between the ZOI of *P. aeruginosa* and *S. aureus* ($p < .05$) when treated with BC-AgZ. This is also the case for both strains ($p < .05$) when treated with BC-$AgNO_3$.

The disc diffusion assay results indicated that BC-$AgNO_3$ had higher antimicrobial activity against *P. aeruginosa* up to 24 h when

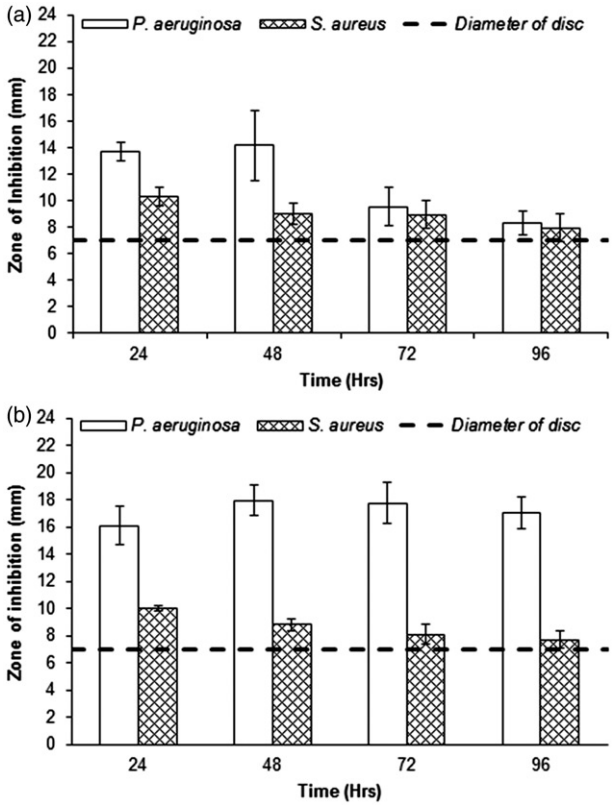

Figure 6. Antimicrobial activity assessed by ZOI during the disc diffusion assay for BC-AgZ loaded under (a) static and (b) constantly agitated conditions against *P. aeruginosa* and *S. aureus* ($n = 6$; error bars = SD).

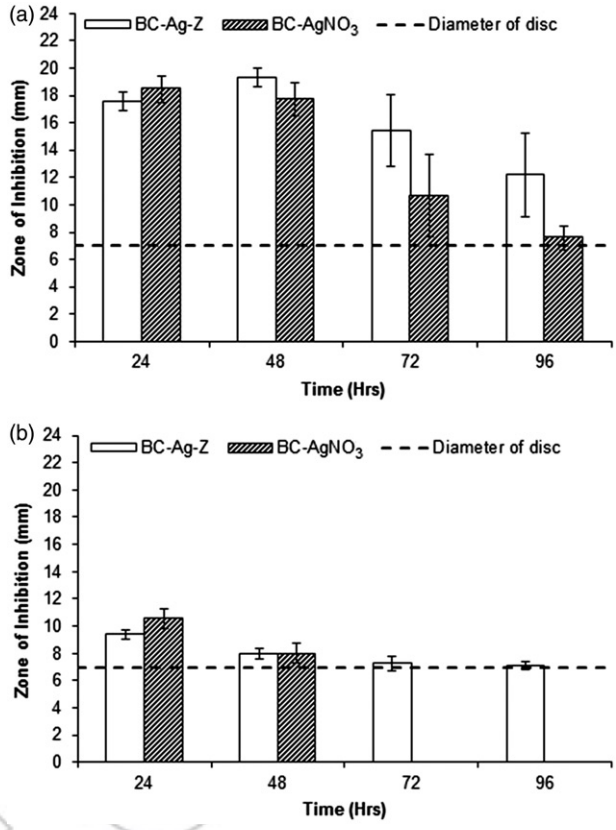

Figure 7. Antimicrobial activity assessed by ZOI during the disc diffusion assay for BC-AgZ and BC-$AgNO_3$ against (a) *P. aeruginosa* and (b) *S. aureus* ($n = 9$; error bars = SD).

compared to BC-AgZ. After 24 h, the antimicrobial activity of BC-$AgNO_3$ reduced and BC-AgZ exhibited higher activity against *P. aeruginosa* (Figure 7(a)). Antimicrobial activity against *S. aureus* also had the same trend at 24 h with BC-$AgNO_3$ exhibiting larger ZOI compared to BC-AgZ. At 48 h, there was no significant difference between BC-$AgNO_3$ and BC-AgZ against *S. aureus*; following incubation at 72 and 96 h, BC-$AgNO_3$ had highly reduced antimicrobial activity against *S. aureus* (ZOI = 0 mm), whereas BC-AgZ still exhibited some antimicrobial activity at 72 h (ZOI = 7.26 ± 0.53 mm), which was further reduced at 96 h (ZOI = 7.11 ± 0.33 mm) (Figure 7(b)). The difference in activity of BC-AgZ and BC-$AgNO_3$ against *P. aeruginosa* (Gram negative) and *S. aureus* (Gram positive) bacteria may be due to their structural differences (see section "Discussion" for details).

Discussion

The concept of moist healing has revolutionised the field of wound management and led to an increased interest in the use of hydrogel-based dressings. In the present study, biosynthetic BC hydrogels were loaded with an Ag^+ donor, $AgNO_3$ or AgZ, and characterised *in vitro* for their application as antimicrobial wound dressings. Once purified, these BC hydrogels become clear and transparent which is advantageous in the management of infected, heavily exudating wounds, as it allows the healing process to be monitored without removing the dressing, hence damaging fragile underlying tissue.

FTIR confirmed that the purified biosynthetic BC hydrogel produced by *G. xylinus* closely resembles commercial cellulose. The broad, characteristic peak at 3328 cm^{-1} falls within the region of 3200–3550 cm^{-1} which is contributed by the stretching of O–H bond (El-Shishtawy et al., 2011). This may also be due to the stretching of the intramolecular hydrogen bond of 3O···H–O5 within the BC network which has been reported to show a characteristic peak at 3348 cm^{-1} (Oh et al., 2005). The narrow peak at 2900 cm^{-1} is due to C–H stretching of CH_2 and CH_3 group, whereas the peak at 1640 cm^{-1} is due to the O–H bending of water molecules (Barud et al., 2008). The peak at 1375 cm^{-1} (C–H bending) provides an indication for the presence of crystalline regions within the BC structure (Castro et al., 2011). Besides that, the peaks at 1159 cm^{-1} (asymmetrical C–O–C bridge stretching) and 1055 cm^{-1} (skeletal vibrations involving C–O stretching) can also be attributed to BC (Barud et al., 2008). The encapsulation of $AgNO_3$ into the BC is confirmed by the occurrence of the specific peaks for Ag at 733 cm^{-1} and 803 cm^{-1} (Valverde-Aguilar et al., 2011). The vibration bands within the region of 1350–400 cm^{-1} are attributed to nitrate ions (NO^{3-}) (Salim and Malik, 2016); hence the presence of a peak at 1370 cm^{-1}, indicates the availability of the nitrate group within BC-$AgNO_3$. The peaks of BC-AgZ at 980 cm^{-1} (asymmetric vibration of Si–O) suggest the presence of a three-dimensional silica phase within the zeolite structure and the peak at 665 cm^{-1} (symmetric stretch) may be contributed by the internal vibrations of the tetrahedral framework (Shameli et al., 2011). FTIR spectra of zeolites reveal the occurrence of a large, intense band at 986 cm^{-1} corresponding to the vibration of the Si–O–Si (Hanim et al., 2016), whereas the peak at 676 cm^{-1} may be due to the bending of Al–O bonds within the zeolite structure (Shameli et al., 2011). Additionally, peaks occurring within the region of 420–500 cm^{-1} may also indicate internal vibrations due to the bending of the T–O tetrahedra, e.g. 477 cm^{-1} corresponding to the internal vibration of (Si, Al)O_4 tetrahedra within the zeolite structure (Karimi-Shamshabadi and Nezamzadeh-Ejhieh, 2016). The presence of silver within the

BC-AgZ network is confirmed by the peak at 553 cm^{-1}, that indicates the Ag–O stretching of AgO and Ag_2O within the 500–600 cm^{-1} region (Waterhouse et al., 2001; Kim et al., 2013).

The swelling ratio of a hydrogel indicates its ability to absorb fluid and is an important property for dressings, especially those used to manage heavily exudating wounds. Hydrogel wound dressings with high degrees of swelling can be applied to a wide variety of wound types, ranging from dry necrotic wounds to full-thickness wounds that produce a high volume of exudate (Kokabi et al., 2007). BC is insoluble in water and most organic solvents, but when immersed in aqueous media its fibrous structure imbibes large amounts of fluid and it swells. The swelling behaviour of this biosynthetic BC hydrogel reveal a high swelling capacity with a swelling ratio of 12.08 ± 0.96 after 24 h, which is in agreement with that reported by other groups (e.g. Nakayama et al., 2004; Maneerung et al., 2008; Wei et al., 2011). The high swelling of BC results from the development of hydrogen bonds with water molecules and the network-like structure of the biopolymer itself that allows BC to imbibe and hold onto those molecules within the crosslinked polymer voids (Maneerung et al., 2008). This high water absorptivity enables BC to maintain a moist environment at the wound site by donating or receiving fluids, thus maintaining an optimal environment in which healing can progress (Lin et al., 2013).

Several methods have been reported for the determination of small molecule antimicrobial release from wound dressings (including metal ions) such as beaker, diffusion cell, paddle over disc and two compartment model (Maneerung et al., 2008; Wei et al., 2011; Jadhav et al., 2012; Peršin et al., 2014; Wu et al., 2014). Each method has unique advantages and disadvantages, and hence no single, standard method has been adopted for the determination of silver release from dressings. In this study, a refined silver release method using 24-well tissue culture flat bottom plates and TSB as release media was developed. At the wound site, silver release from dressings is dependent on several factors including the type of wound, classification and size of dressing, volume of exudate, etc. The authors are mindful that the method designed and employed for the determination of silver release in the current study may not exactly mirror the real wound environment; for that to occur the presence of phagocytes, inflammatory mediators, hydrolytic enzymes, reactive oxygen species, bacteria and their associated by-products would need to be considered (Ovington, 2007; Martin et al., 2013). Nevertheless, this method has several advantages due to its simplicity, low cost and biorelevant temperature conditions. Silver release, as quantified by ICP indicated that the Ag^+ zeolite-loaded hydrogels (BC-AgZ) released more Ag^+ than their $AgNO_3$ counterparts (BC-$AgNO_3$). The microporous zeolite framework allows greater initial Ag^+ loading and a subsequent ion-exchange mediated release of biologically active Ag^+ into the surrounding medium (Kwakye-Awuah et al., 2008).

These experiments revealed that BC loaded under conditions of constant agitation demonstrated greater antimicrobial activity, compared to the statically loaded hydrogels. This may be due to the more evenly distributed Ag^+ loading under agitated condition as compared to static incubation, which contributed to a more consistent release of Ag^+ (Figure 2(c,d)).

The prolonged antimicrobial activity exhibited by BC-AgZ against both *P. aeruginosa* and *S. aureus* resulted from the controlled release of Ag^+ from the zeolite structure. Zeolites are crystalline aluminosilicate cages with cavities occupied by cations or water molecules. The AgZ acts as an inorganic reservoir and silver in the zeolite have considerable freedom of movements (Kwakye-Awuah et al., 2008). In addition to the ionic exchange-based release of Ag^+ encapsulated within the zeolite, BC matrix was able to provide a second layer of controlled release. In contrast, release of Ag^+ from BC-$AgNO_3$ was only controlled by the BC matrix, hence Ag^+ release was less prolonged when compared to BC-AgZ.

Results revealed that both BC-AgZ and BC-$AgNO_3$ exhibited antimicrobial activity against the Gram positive and Gram negative strains tested, but that activity was stronger and more prolonged against *P. aeruginosa* compared to *S. aureus*. Ag^+ has strong bactericidal activity (Copcia et al., 2011), and Gram negative bacteria are more susceptible to Ag^+ than the Gram positive species (Ip et al., 2006; Waghmare et al., 2015) due to differences in their cell wall structure and composition. The Gram positive bacterial cell wall contains a thicker peptidoglycan layer than that of Gram negative strains. Gram positive bacterial cell walls typically lack an outer membrane and are mainly composed of a thick, negatively charged peptidoglycan layer and cytoplasmic phospholipid bilayer. Contrary to this, Gram negative microorganisms have a thin (≈2–3 nm) peptidoglycan layer between the outer membrane and the cytoplasmic phospholipid bilayer (Le et al., 2010). The composition of the peptidoglycan layer, which contains teichoic acids, contributes to the overall anionic charge of the Gram positive cell surface (Neuhaus and Baddiley, 2003); this greater net anionic charge may bind more Ag^+, thus reducing the amount that can reach the plasma membrane and intracellular targets to exert their antimicrobial activity. This finding is in agreement with Le et al. (2010) who reported that *E. coli* (Gram negative) was more sensitive to the effects of silver nanoparticles (versus *S. aureus*, a Gram positive) because of differences in the thickness of the peptidoglycan layer (Le et al., 2010). Gram negative microorganisms are generally less sensitive to antibiotics and certain antimicrobial agents due to the selective permeability and protective mechanism of their outer membrane structure (Bomberger et al., 2009; Sperandeo et al., 2009). Nevertheless, Ag^+ has shown its ability to exert microbiocidal activity against a variety of pathogenic microorganisms, including drug resistant strains. In addition, its multi-target antimicrobial activities are advantageous in limiting the potential development of resistant microbial strains (Brett, 2006; Radecka et al., 2015). Hence the development of a responsive, topical silver formulation would be extremely useful for the treatment of infected chronic wounds.

Conclusions

The present study demonstrates the *in vitro* stability, performance and antimicrobial potential of biosynthetic BC hydrogels loaded with $AgNO_3$ or AgZ against representative wound infecting microorganisms (*P. aeruginosa* and *S. aureus*). The moist and responsive nature of BC hydrogels make them an ideal biomaterial dressing for the management of chronic, infected wounds. Further research aims to optimise the performance of BC hydrogels loaded with microencapsulated silver to provide a responsive, controlled release delivery platform, whilst minimising the toxicity associated with localised high concentrations of topical silver.

Disclosure statement

The authors report no conflicts of interest. The authors alone are responsible for the content and writing of the article.

ORCID

Claire Martin http://orcid.org/0000-0002-5497-4594

References

Abdelrahman T, Newton H. Wound dressings: Principles and practices. Surgery, 2011;29(10):491–5.

Abeer MM, Amin MCIM, Martin C. A review of bacterial cellulose-based drug delivery systems: Its' biochemistry, current approaches and future prospects. J Pharm Pharmacol, 2014;66(8):1047–61.

Atiyeh BS, Costagliola M, Hayek SN, Dibo SA. Effect of silver on burn wound infection control and healing: Review of the literature. Burns, 2007;33(2):139–48.

Barud HS, Assunção RMN, Martines MAU, Dexpert-Ghys J, Marques RFC, Messaddeq Y, Ribeiro SJL. Bacterial cellulose–silica organic–inorganic hybrids. J Sol–Gel Sci Technol, 2008;46(3):363–7.

Bomberger JM, MacEachran DP, Coutermarsh BA, Ye S, O'Toole GA, Stanton BA. Long-distance delivery of bacterial virulence factors by *Pseudomonas aeruginosa* outer membrane vesicles. PLoS Pathog, 2009;5(4):e1000382 [online] Available at: http://journals.plos.org/plospathogens/article?id=10.1371/journal.ppat.1000382.

Brett DW. A discussion of silver as an antimicrobial agent: Alleviating the confusion. Ostomy/Wound Manage, 2006;52(1):34–41.

Castellano JJ, Shafii SM, Ko F, Donate G, Wright TE, Mannari RJ, Payne WG, Smith DJ, Robson MC. Comparative evaluation of silver-containing antimicrobial dressings and drugs. Int Wound J, 2007;4(2):114–22.

Castro C, Zuluaga R, Putaux JL, Caro G, Mondragon I, Ganán P. Structural characterization of bacterial cellulose produced by *Gluconacetobacter swingsii* sp. from Colombian agroindustrial wastes. Carbohydr Polym, 2011;84(1):96–102.

Chopra I. The increasing use of silver-based products as antimicrobial agents: A useful development or a cause for concern? J Antimicrob Chemother, 2007;59(4):587–90.

Copcia VE, Luchian C, Dunca S, Bilba N, Hristodor CM. Antibacterial activity of silver-modified natural clinoptilolite. J Mater Sci, 2011;46(22):7121–8.

Costa P, Lobo JMS. Modeling and comparison of dissolution profiles. Eur J Pharm Sci, ~~2011~~;13(2):123–33.

Czaja W, Krystynowicz A, Bielecki S, Brown MB. Microbial cellulose – the natural power to heal wounds. Biomaterials, 2006;27(2):145–51.

Dash S, Murthy PN, Nath L, Chowdhury P. Kinetic modeling on drug release from controlled drug delivery systems. Acta Pol Pharm. Drug Res, 2010;67(3):217–23.

El-Shishtawy RM, Asiri AM, Abdelwahed NA, Al-Otaibi MM. In situ production of silver nanoparticle on cotton fabric and its antimicrobial evaluation. Cellulose, 2011;18(1):75–82.

Fu L, Zhang J, Yang G. Present status and applications of bacterial cellulose-based materials for skin tissue repair. Carbohydr Polym, 2013;92(2):1432–42.

Guo S, DiPietro LA. Factors affecting wound healing. J Dent Res, 2010;89(3):219–29.

Hanim SAM, Malek NANN, Ibrahim Z. Amine-functionalized, silver-exchanged zeolite NaY: Preparation, characterization and antibacterial activity. Appl Surf Sci, 2016;360(Part A):121–30.

Hestrin S, Schramm M. Synthesis of cellulose by *Acetobacter xylinum*. 2. Preparation of freeze-dried cells capable of polymerizing glucose to cellulose. Biochem J, 1954;58(2):345–52.

Ip M, Lui SL, Poon VK, Lung I, Burd A. Antimicrobial activities of silver dressings: An *in vitro* comparison. J Med Microbiol, 2006;55(Pt 1):59–63.

Jadhav H, Joshi A, Misra M, Shahiwala A. Effects of various formulation parameters on the properties of hydrogel wound dressings. Drug Deliv Lett, 2012;2(1):8–13.

Kamoun EA, Chen X, Eldin MSM, Kenawy E-R. Crosslinked poly(vinyl alcohol) hydrogels for wound dressing applications: A review of remarkably blended polymers. Arab J Chem, 2015;8(1):1–14.

Karimi-Shamsabadi M, Nezamzadeh-Ejhieh A. Comparative study on the increased photoactivity of coupled and supported manganese-silver oxides onto a natural zeolite nano-particles. J Mol Catal A: Chem, 2016;418–419:103–14.

Kim J, Kwon S, Ostler E. Antimicrobial effect of silver-impregnated cellulose: Potential for antimicrobial therapy. J Biol Eng, 2009;3(20) [online] doi:10.1186/1754-1611-3-20. Available at: http://www.jbioleng.org/content/3/1/20.

Kim PS, Kim MK, Cho BK, Nam IS, Oh SH. Effect of H_2 on deNOx performance of HC-SCR over Ag/Al_2O_3: Morphological, chemical, and kinetic changes. J Catal, 2013;301:65–76.

Kirketerp-Møller K, Jensen PO, Fazli M, Madsen KG, Pedersen J, Moser C, Tolker-Nielsen T, Høiby N, Givskov M, Bjarnsholt T. Distribution, organization and ecology of bacteria in chronic wound. J Clin Microbiol, 2008;46(8):2717–22.

Kokabi M, Sirousazar M, Hassan ZM. PVA–clay nanocomposite hydrogels for wound dressing. Eur Polym J, 2007;43(3):773–81.

Kwakye-Awuah B, Wemegah DD, Nkrumah I, Williams C, Radecka I. Antimicrobial activity of silver-zeolite LTA on heavily-contaminated underground Ghanaian waters. Int J Sci Res, 2013;2(11):26–31.

Kwakye-Awuah B, Williams C, Kenward MA, Radecka I. Antimicrobial action and efficiency of silver-loaded zeolite X. J Appl Microbiol, 2008;104(5):1516–24.

Landis SJ. Chronic wound infection and antimicrobial use. Adv Skin Wound Care, 2008;21(11):531–40.

Le AT, Tam LT, Tam PD, Huy PT, Huy TQ, Hieu NV, Kudrinskiy AA, Krutyakov YA. Synthesis of oleic acid-stabilized silver nanoparticles and analysis of their antibacterial activity. Mater Sci Eng: C, 2010;30(6):910–16.

Leaper D. Appropriate use of silver dressings in wounds: International consensus document. Int Wound J, 2012;9(5):461–4.

Lin WC, Lien CC, Yeh HJ, Yu CM, Hsu SH. Bacterial cellulose and bacterial cellulose-chitosan membranes for wound dressing applications. Carbohydr Polym, 2013;94(1):603–11.

Low WL, Martin C, Hill DJ, Kenward MA. Antimicrobial efficacy of silver ions in combination with tea tree oil against *Pseudomonas aeruginosa, Staphylococcus aureus* and *Candida albicans*. Int J Antimicrob Agents, 2011;37(2):162–5.

Low WL, Martin C, Hill DJ, Kenward MA. Antimicrobial efficacy of liposome encapsulated silver ions and tea tree oil against *Pseudomonas aeruginosa, Staphylococcus aureus* and *Candida albicans*. Lett Appl Microbiol, 2013;57(1):33–9.

Maneerung T, Tokura S, Rujiravanit R. Impregnation of silver nanoparticles into bacterial cellulose for antimicrobial dressing. Carbohydr Polym, 2008;72(1):43–51.

Martin C, Low WL, Amin MCIM, Radecka I, Raj P, Kenward MA. Current trends in the development of wound dressings, biomaterials and devices. Pharm Patent Anal, 2013;2(3):341–59.

Martin C, Low WL, Gupta A, Amin MCIM, Radecka I, Britland ST, Raj P, Kenward MA. 2014. Liposomal delivery of antimicrobials. In: Finney L, ed. Advances in liposome research (part of the Biochemistry Research Trends Series). New York, USA: Nova Science Publishers Inc., pp. 27–62.

Martin C, Low WL, Gupta A, Amin MCIM, Radecka I, Britland ST, Raj P, Kenward MA. Strategies for antimicrobial drug delivery to biofilm. Curr Pharm Des, 2015;21(1):43–66.

Matsumura Y, Yoshikata K, Kunisaki SI, Tsuchido T. Mode of bactericidal action of silver zeolite and its comparison with that of silver nitrate. Appl Environ Microbiol, 2003;69(7):4278–81.

Murphy PS, Evans GRD. Advances in wound healing: A review of current wound healing products. Plast Surg Int, 2012;2012: Article ID 190436, doi:10.1155/2012/190436.

Nakayama A, Kakugo A, Gong JP, Osada Y, Takai M, Erata T, Kawano S. High mechanical strength double-network hydrogel with bacterial cellulose. Adv Funct Mater, 2004;14(11):1124–8.

Neuhaus FC, Baddiley J. A continuum of anionic charge: Structures and functions of d-alanyl-teichoic acids in Gram-positive bacteria. Microbiol Mol Biol Rev, 2003;67(4):686–723.

Oh SY, Yoo DI, Shin Y, Kim HC, Kim HY, Chung YS, Park WH, Youk JH. Crystalline structure analysis of cellulose treated with sodium hydroxide and carbon dioxide by means of X-ray diffraction and FTIR spectroscopy. Carbohydr Res, 2005;340(15):2376–91.

Ovington LG. Advances in wound dressings. Clin Dermatol, 2007;25(1):33–8.

Peršin Z, Maver U, Pivec T, Maver T, Vesel A, Mozetič M, Stana-Kleinschek K. Novel cellulose based materials for safe and efficient wound treatment. Carbohydr Polym, 2014;100:55–64.

Pinto RJ, Marques PA, Neto CP, Trindade T, Daina S, Sadocco P. Antibacterial activity of nanocomposites of silver and bacterial or vegetable cellulosic fibers. Acta Biomater, 2009;5(6):2279–89.

Radecka I, Martin C, Hill DJ. 2015. The problem of microbial drug resistance. In*:* Phoenix DA, Harris F, Dennison SR, eds. Novel antimicrobial agents and strategies. Weinheim, Germany: Wiley-VCH, pp. 1–16.

Salim MM, Malek NANN. Characterization and antibacterial activity of silver exchanged regenerated NaY zeolite from surfactant-modified NaY zeolite. Mater Sci Eng: C, 2016;59:70–7.

Sannino A, Demitri C, Madaghiele M. Biodegradable cellulose-based hydrogels: Design and applications. Materials, 2009;2(2): 353–73.

Shah N, Ul-Islam M, Khattak WA, Park JK. Overview of bacterial cellulose composites: A multipurpose advanced material. Carbohydr Polym, 2013;98(2):1585–98.

Shameli K, Ahmad MB, Zargar M, Yunus WMZW, Ibrahim NA. Fabrication of silver nanoparticles doped in the zeolite framework and antibacterial activity. Int J Nanomed, 2011;6:331–41.

Singh B, Sharma S, Dhiman A. Design of antibiotic hydrogel wound dressing: Biomedical properties and histological study of wound healing. Int J Pharm, 2013;457(1):82–91.

Solway DR, Fapwca F, Consalter M, Levinson DJ. Microbial cellulose wound dressing in the treatment of skin tears in the frail elderly. Wounds, 2010;22(1):17–19.

Sperandeo P, Dehò G, Polissi A. The lipopolysaccharide transport system of Gram-negative bacteria. Biochim Biophys Acta (BBA)-Mol Cell Biol Lipids, 2009;1791(7):594–602.

Valverde-Aguilar G, García-Macedo JA, Rentería-Tapia VM, Gómez RW, Quintana-García M. Modelling of optical absorption of silver NP's produced by UV radiation embedded in mesostructured silica films. J Nanopart Res, 2011;13(10):4613–22.

Waghmare SR, Mustopa NM, Suryakant RM, Kailas DS. Ecofriendly production of silver nanoparticles using *Candida utilis* and its mechanistic action against pathogenic microorganisms. 3 Biotech, 2015;5(1):33–8.

Waterhouse GI, Bowmaker GA, Metson JB. The thermal decomposition of silver (I, III) oxide: A combined XRD, FT-IR and Raman spectroscopic study. Phys Chem Chem Phys, 2001;3(17):3838–45.

Wei B, Yang G, Hong F. Preparation and evaluation of a kind of bacterial cellulose dry films with antibacterial properties. Carbohydr Polym, 2011;84(1):533–8.

Wilkinson LJ, White RJ, Chipman JK. Silver and nanoparticles of silver in wound dressings: A review of efficacy and safety. J Wound Care, 2011;20(11):543–9.

Winter GD. Formation of the scab and rate of epithelialization of superficial wounds in the skin of the young domestic pig. Nature, 1962;193:293–4.

Wu J, Zheng Y, Song W, Luan J, Wen X, Wu Z, Chen X, Wang Q, Guo S. *In situ* synthesis of silver-nanoparticles/bacterial cellulose composites for slow-released antimicrobial wound dressing. Carbohydr Polym, 2014;102:762–71.

Yang G, Xie J, Hong F, Cao Z, Yang X. Antimicrobial activity of silver nanoparticle impregnated bacterial cellulose membrane: Effect of fermentation carbon source of bacterial cellulose. Carbohydr Polym, 2012;87(1):839–45.